The computation aspects of the equivalent-layer technique: review and perspective

Diego Takahashi [1,*], André L. A. Reis [2], Vanderlei C. Oliveira Jr. [1] and Valéria C. F. Barbosa [1]

[1] *Observatório Nacional, Department of Geophysics, Rio de Janeiro, Brasil*
[2] *Universidade do Estado do Rio de Janeiro, Department of Applied Geology, Rio de Janeiro, Brasil*

Correspondence*:
Valéria C.F. Barbosa
valcris@on.br

ABSTRACT

Equivalent-layer technique is a powerful tool for processing potential-field data in the space domain. However, the greatest hindrance for using the equivalent-layer technique is its high computational cost for processing massive data sets. The large amount of computer memory usage to store the full sensitivity matrix combined with the computational time required for matrix-vector multiplications and to solve the resulting linear system, are the main drawbacks that made unfeasible the use of the equivalent-layer technique for a long time. More recently, the advances in computational power propelled the development of methods to overcome the heavy computational cost associated with the equivalent-layer technique. We present a comprehensive review of the computation aspects concerning the equivalent-layer technique addressing how previous works have been dealt with the computational cost of this technique. Historically, the high computational cost of the equivalent-layer technique has been overcome by using a variety of strategies such as: moving data-window scheme, equivalent data concept, wavelet compression, lower-dimensional subspace, quadtree discretization, reparametrization of the equivalent layer by a piecewise-polynomial function, iterative scheme without solving a system of linear equations and the convolutional equivalent layer using the concept of block-Toeplitz Toeplitz-block (BTTB) matrices. We compute the number of floating-point operations of some of these strategies adopted in the equivalent layer technique to show their effectiveness in reducing the computational demand. Numerically, we also address the stability of some of these strategies used in the equivalent layer technique by comparing with the stability via the classic equivalent-layer technique with the zeroth-order Tikhonov regularization.

Keywords: equivalent layer, gravimetry, fast algorithms, computational cost, stability analysis

1 INTRODUCTION

In accord with potential theory, a continuous potential-field data (gravity and magnetic data) produced by any source can be exactly reproduced by a continuous and infinite 2D physical-property surface distribution that is called the equivalent layer. The equivalent layer is a mathematical solution of Laplace's equation in the source-free region with the observed potential-field data as the Dirichlet boundary condition (Kellogg, 1929). Grounded on well-established potential theory, the equivalent-layer technique has been used by exploration geophysicists for processing potential-field data since the late 1960s (Dampney, 1969).

Although there was always a great demand for gravity and magnetic data processing, the equivalent-layer technique has not been massively used. This occurs because its high computational cost makes the equivalent-layer technique computationally inefficient for processing massive data sets. In the classic equivalent-layer technique, the continuous problem of the equivalent layer involving integrals is approximated by a discrete form of the equivalent layer. First, a discrete and finite set of equivalent sources (point masses, prisms, magnetic diploes, doublets) is arranged in a layer with finite horizontal dimensions and located below the observation surface. Next, a linear system of equations is set up with a large and full sensitivity matrix. Then, a regularized linear inverse problem is solved to estimate the physical property of each equivalent source within the discrete equivalent layer subject to fitting a discrete set of potential-field observations. Finally, the estimated physical-property distribution within the equivalent layer is used to accomplish the desired processing of the potential-field data (e.g., interpolation, upward/downward continuation, reduction to the pole). The latter step is done by multiplying the matrix of Green's functions associated with the desired transformation by the estimated physical-property distribution.

Beginning in the late 1980s, the equivalent-layer techniques computationally efficient have arose. To our knowledge, the first method towards improving the efficiency was proposed by Leão and Silva (1989) who used an overlapping moving-window scheme spanning the data set. The strategy adopted in Leão and Silva (1989) involves solving several smaller, regularized linear inverse problems instead of one large problem. This strategy uses a small data window and distributes equivalent sources on a small regular grid at a constant depth located below the data surface. Leão and Silva (1989) ensure that sources window extends beyond the boundaries of the data window. For each position of the data window, this scheme consists in computing the processed field at the center of the data window only and the next estimates of the processed field are obtained by shifting the data window across the entire dataset. Recently, Soler and Uieda (2021) developed a computational approach to increase the efficiency of the equivalent-layer techinique by combining two strategies. The fisrt one — the block-averaging source locations — reduces the model parameters and the second strategy — the gradient-boosted algorithm — reduces the size of the linear system to be solved by fitting the equivalent source model iteratively along overlapping windows. Notice that the equivalent-layer strategy of using a moving-window scheme either in Leão and Silva (1989) or in Soler and Uieda (2021) is similar to discrete convolution.

In another approach to reduce computational workload of the equivalent-layer technique Mendonça and Silva (1994) developed an iterative procedure by incorporating one data point at a time and thus selecting a smaller data set. This strategy adopted by Mendonça and Silva (1994) is known as 'equivalent data concept'. Li and Oldenburg (2010) transformed the full sensitivity matrix into a sparse one using the compression of the coefficient matrix via wavelet transforms based on the orthonormal compactly supported wavelets. For jointly processing the components of gravity-gradient data using the equivalent-source processing, Barnes and Lumley (2011) applied the quadtree model discretization to generate a sparse linear system of equations. Davis and Li (2011) adaptively dicretized the model (quadtree model discretization) based on localized anomalies and used wavelet transforms to reduce, reordered the model parameters (Hilbert space-filling curves) and compressed each row of the sensitivity matrix of the reordered parameter set (wavelet transforms). By using the subspace method, Mendonça (2020) reduced the dimension of the linear system of equations to be solved in the equivalent-layer technique. The subspace bases span the parameter-model space and they are constructed by applying the singular value decomposition to the matrix containing the gridded data. These strategies followed by Li and Oldenburg (2010), Barnes and Lumley (2011), Davis and Li (2011) and Mendonça (2020) may be grouped into the strategy of compression approaches to solve large linear system of equations.

Following the strategy of reparametrization of the equivalent layer, Oliveira Jr. et al. (2013) reduced the model parameters by approximating the equivalent-source layer by a piecewise-polynomial function defined on a set of user-defined small equivalent-source windows. The estimated parameters are the polynomial coefficients for each window and they are much smaller than the original number of equivalent sources. Siqueira et al. (2017) developed an iterative solution where the sensitivity matrix is transformed into a diagonal matrix with constant terms through the use of the 'excess mass criterion' and of the positive correlation between the observed gravity data and the masses on the equivalent layer. Jirigalatu and Ebbing (2019) combined the Gauss-fast Fourier transform (FFT) with Landweber's algorithm and proposed a fast equivalent-layer technique for jointly processing two-components of the gravity-gradient data. The Landweber's algorithm has some similarities with with gradient-descent algorithm. The strategies worked out by Siqueira et al. (2017) and Jirigalatu and Ebbing (2019) avoid calculating the Hessian matrix and solving linear system of equations.

Recently, Takahashi et al. (2020, 2022), developed fast and effective equivalent-layer techniques for processing, respectively, gravity and magnetic data by modifying the forward modeling to estimate the physical-property distribution over the layer through a 2D discrete convolution that can be efficiently computed via 2D FFT. These methods took advantage of the Block-Toeplitz Toeplitz-block (BTTB) structure of the sensitivity matrices, allowing them to be calculated by using only their first column. In practice, the forward modeling uses a single equivalent source, which significantly reduces the the required RAM memory. Takahashi et al. (2020, 2022) employed the strategy of the convolutional equivalent layer using the concept of BTTB matrices.

Here, we present a comprehensive review of

2 THE EQUIVALENT-LAYER TECHNIQUE

2.1 Fundamentals

Consider a set of N potential-field observations (gravity or magnetic data) $d_i^o\ (x_i, y_i, z_i)$, $i = 1, \ldots, N$, at the ith observation point (x_i, y_i, z_i) of a Cartesian coordinate system with x-, y- and z-axis pointing to north, east and down, respectively. Physically, the discrete set of potential-field observations is produced by a unknown source distribution in the subsurface. Mathematically, it represents a discrete set of a harmonic function.

A standard way to deal with the classical equivalent-layer technique is approximate the observed potential-field data by the predicted data, which in turn are produced by a fictitious layer of sources, called equivalent layer. The equivalent layer is located below the observation surface, at depth z_0 ($z_0 > z_i$), and with finite horizontal dimensions being composed by a finite discrete set of equivalent sources (e.g., point masses, dipoles, or prisms). Mathematically, this approximation can be written in matrix notation as

$$\mathbf{d} = \mathbf{A}\mathbf{p}\,, \tag{1}$$

where $\mathbf{d}$ is an N-dimensional predicted data vector whose ith element, $d_i\ (x_i, y_i, z_i)$, $i = 1, \ldots, N$, is the predicted potential-field observation, $\mathbf{p}$ is an M-dimensional parameter vector whose jth element p_j is a physical property of the jth equivalent source and $\mathbf{A}$ is the $N \times M$ sensitivity matrix whose ijth element a_{ij} is a harmonic function.

2.2 Computational strategies

The classical equivalent-layer technique consists of estimating the parameter vector $\mathbf{p}$ from the N-dimensional observed data vector $\mathbf{d^o}$ whose ith element is defined as the $d_i^o\ (x_i, y_i, z_i)$, $i = 1, \ldots, N$. Usually, this estimate can be obtained by a regularized least-squares solution The estimated parameter is stable, fits the observed data and can be used to yield a desired linear transformation of the data, such as interpolation, upward (or downward) continuation, reduction to the pole, joint processing of gravity gradient data and more. Mathematically, the desired linear transformation of the data can be obtained by

$$\hat{\mathbf{t}} = \mathbf{T}\mathbf{p}^*\,, \tag{2}$$

where $\hat{\mathbf{t}}$ is an N-dimensional transformed data vector, $\mathbf{p}^*$ is an M-dimensional estimated parameter vector and $\mathbf{T}$ is the $N \times M$ matrix of Green's functions whose ijth element is the transformed field at the ith observation point produced by the jth equivalent source.

The biggest hurdle to use the classical equivalent-layer technique is the computational complexity to handle large datasets because the sensitivity matrix $\mathbf{A}$ (equation 1) is dense. Usually, the estimated parameter vector $\mathbf{p}^*$ requires to solve a large-scale linear inversion which in turn means to deal with some obstacles concerning large computational cost: i) the large computer memory to store large and full matrices; ii) the long computation time to mutiply a matrix by a vector; and iii) the long computation time to solve a large linear system of equations.

Here, we review some strategies for reducing the computational cost of equivalent-layer technique. These strategies are the following:

2.2.1 The moving data-window scheme

Leão and Silva (1989) reduced the total processing time and memory usage of equivalent-layer technique by means of a moving data-window scheme. A small moving data window with N_w observations and a small equivalent layer with M_w equivalent sources ($M_w > N_w$) located below the observations are established. For each position of a moving-data window, Leão and Silva (1989) estimate a stable solution $\mathbf{p}^*$ by using a data-space approach with the zeroth-order Tikhonov regularization (Aster et al., 2018), i.e.,

$$\mathbf{p}^* = \mathbf{A}^\top \left(\mathbf{A}\mathbf{A}^\top + \mu \mathbf{I} \right)^{-1} \mathbf{d}^o \, , \tag{3}$$

where μ is a regularizing parameter, $\mathbf{I}$ is an identity matrix of order N_w and the superscript $\top$ stands for a transpose. After estimating an $M_w \times 1$ parameter vector $\mathbf{p}^*$ (equation 3) the desired transformation of the data is only calculated at the central point of each moving-data window, i.e.:

$$\hat{t}_k = \mathbf{t}_k^\top \, \mathbf{p}^* \, , \tag{4}$$

where $\hat{t}_k$ is the transformed data calculated at the central point k of the data window and $\mathbf{t}_k$ is an $M1$ vector whose elements form the kth row of the matrix of Green's functions $\mathbf{T}$ (equation 2) of the desired linear transformation of the data.

By shifting the moving-data window with a shift size of one data spacing, a new position of a data window is set up. Next, the aforementioned process (equations 3 and 4) is repeated for each position of a moving-data window, until the entire data have been processed. Hence, instead of solving a large inverse problem, Leão and Silva (1989) solve several much smaller ones.

To reduce the size of the linear system to be solved, Soler and Uieda (2021) adopted the same strategy proposed, originally, by Leão and Silva (1989) of using a small moving-data window sweeping the whole data. In Leão and Silva (1989), a moving-data window slides to the next adjacent data window following a sequential movement, the predicted data is calculated inside the data window and the desired transformation are only calculated at the center of the moving-data window. Unlike Leão and Silva (1989), Soler and Uieda (2021) do not adopt a sequential order of the data windows; rather, they adopt a randomized order of windows in the iterations of the gradient-boosting algorithm (Friedman, 2001 and 2002). The gradient-boosting algorithm in Soler and Uieda (2021) estimates a stable solution using the data and the equivalent sources that fall within a moving-data window; however, it calculates the predicted data and the residual data in the whole survey data. Next, the residual data that fall within a new position of the data window is used as input data to estimate a new stable solution within the data window which in turn is used to calculated a new predicted data and a new residual data in the whole survey data. Finally, unlike Leão and Silva (1989), in Soler and Uieda (2021) neither the data nor the equivalent sources need to be distributed in regular grids. Indeed, Leão and Silva (1989) built their method using regular grids, but in fact regular grids are not necessary. Regarding the equivalent-source layout, Soler and Uieda (2021) proposed the block-averaged sources locations in which the survey area is divided into horizontal blocks and one single equivalent source is assigned to each block. Each single source per block is placed over the layer with its horizontal coordinates given by the average horizontal positions of observation points. According to Soler and Uieda (2021), the block-averaged sources layout reduces the number of equivalent sources significantly and the gradient-boosting algorithm provides even greater efficiency in terms of data fitting.

2.2.2 The equivalent-data concept

To reduced the total processing time and memory usage of equivalent-layer technique, Mendonça and Silva (1994) proposed a strategy called 'equivalent data concept'. The equivalent data concept is grounded on the principle that there is a subset of redundant data that does not contribute to the final solution and thus can be dispensed. Conversely, there is a subset of observations, called equivalent data, that contributes effectively to the final solution and fits the remaining observations (redundant data). Iteractively, Mendonça and Silva (1994) selected the subset of equivalent data that is substantially smaller than the original dataset. This selection is carried out by incorporating one data point at a time.

According to Mendonça and Silva (1994), the number of equivalent data is about one-tenth of the total number of observations. These authors used the equivalent data concept to carry out an interpolation of gravity data. They showed a reduction of the total processing time and memory usage by, at least, two orders of magnitude as opposed to using all observations in the interpolation process via the classical equivalent-layer technique.

2.2.3 The wavelet compression and lower-dimensional subspace

For large data sets, the sensitivity matrix $\mathbf{A}$ (equation 1) is a drawback in applying the equivalent-layer technique because it is a large and dense matrix.

Li and Oldenburg (2010) transformed a large and full sensitivity matrix into a sparse one by using fast wavelet transforms. In the wavelet domain, Li and Oldenburg (2010) applyied a 2D wavelet transform to each row and column of the original sensitivity matrix $\mathbf{A}$ to expand it in the wavelet bases. This operation can be done by premultiplying the original sensitivity matrix $\mathbf{A}$ by a matrix representing the 2D wavelet transform $\mathbf{W_2}$ and then the resulting is postmultiplied by the transpose of $\mathbf{W_2}$ (i.e., $\mathbf{W_2}^\top$).

$$\tilde{\mathbf{A}} = \mathbf{W_2}\, \mathbf{A}\, \mathbf{W_2}^\top \,, \tag{5}$$

where $\tilde{\mathbf{A}}$ is the expanded original sensitivity matrix in the wavelet bases with many elements zero or close to zero. Next, the matrix $\tilde{\mathbf{A}}$ is replaced by its sparse version $\tilde{\mathbf{A}}_\mathbf{s}$ in the wavelet domain which in turn is obtained by retaining only the large elements of the $\tilde{\mathbf{A}}$. Thus, the elements of $\tilde{\mathbf{A}}$ whose amplitudes fall below a relative threshold are discarded. In Li and Oldenburg (2010), the original sensitivity matrix $\mathbf{A}$ is high compressed resulting in a sparce matrix $\tilde{\mathbf{A}}_\mathbf{s}$ with a few percent of nonzero elements and the regularized inverse problem is solved in the wavelet domain by using $\tilde{\mathbf{A}}_\mathbf{s}$. Finally, the equivalent source, in the space domain, is obtained by applying an inverse wavelet transform. For regularly spaced grid of data, Li and Oldenburg (2010) reported that high compression ratios are achived with insignificant loss of accuracy.

Li and Oldenburg (2010) used the equivalent-layer technique with a wavelet compression to perform an upward continuation of total-field anomaly between uneven surfaces. As compared to the upward-continued total-field anomaly by equivalent layer using the dense matrix, Li and Oldenburg's (2010) approach, using the Daubechies wavelet, decreased CPU (central processing unit) time by up to two orders of magnitude.

Mendonça (2020) overcame the solution of intractable large-scale equivalent-layer problem by using the subspace method (e.g., Skilling and Bryan, 1984; Kennett et al., 1988; Oldenburg et al., 1993; Barbosa et al., 1997). The subspace method reduces the dimension of the linear system of equations to be solved. Given a higher-dimensional space (e.g., M-dimensional model space, $\mathbb{R}^M$), there exists many lower-dimensional subspaces (e.g., Q-dimensional subspace) of $\mathbb{R}^M$. The linear inverse problem related to the equivalent-layer technique consists in finding an M-dimension parameter vector $\mathbf{p} \in \mathbb{R}^M$ which adequately fits the potential-field data. The subspace method looks for a parameter vector who lies in a Q-dimensional subspace of $\mathbb{R}^M$ which, in turn, is spanned by a set of Q vectors $\mathbf{v}_i = 1, ..., Q$, where $\mathbf{v}_i \in \mathbb{R}^M$ In matrix notation, the parameter vector in the subspace method can be written as

$$\mathbf{p} = \mathbf{V}\, \boldsymbol{\alpha} \,, \tag{6}$$

where $\mathbf{V}$ is an $M \times Q$ matrix whose columns $\mathbf{v}_i = 1, ..., Q$ form a basis vectors for a subspace Q of $\mathbb{R}^M$. In equation 6, the parameter vector $\mathbf{p}$ is defined as a linear combination in the space spanned by Q basis vectors $\mathbf{v}_i = 1, ..., Q$ and α is a Q-dimensional unknown vector to be determined. The main advantage of the subspace method is that the linear system of M equations in M unknowns to be originally solved is reduced to a new linear system of Q equations in Q unknowns which requires much less computational effort since $Q << M$. The choice of the Q basis vectors $\mathbf{v}_i = 1, ..., Q$ (equation 6) in the subspace method is not strict. Mendonça (2020), for example, chose the eigenvectors yielded by applying the singular value decomposition of the matrix containing the gridded data set. The number of eigenvectors used to form basis vectors will depend on the singular values.

The proposed subspace method for solving large-scale equivalent-layer problem by Mendonça (2020) was applied to estimate the mass excess or deficiency caused by causative gravity sources.

2.2.4 The quadtree discretization

To make the equivalent-layer technique tractable, Barnes and Lumley (2011) also transformed the dense sensitivity matrix $\mathbf{A}$ (equation 1) into a sparse matrix. In Barnes and Lumley (2011), a sparce version of the sensitivity matrix is achived by grouping equivalent sources (e.g., they used prisms) distant from an observation point together to form a larger prism or larger block. Each larger block has averaged physical properties and averaged top- and bottom-surfaces of the grouped smaller prisms (equivalent sources) that are encompassed by the larger block. The authors called it the 'larger averaged block' and the essence of their method is the reduction in the number of equivalent sources, which means a reduction in the number of parameters to be estimated implying in model dimension reduction.

The key of the Barnes and Lumley's (2011) method is the algorithm for deciding how to group the smaller prisms. In practice, these authors used a recursive bisection process that results in a quadtree discretization of the equivalent-layer model.

By using the quadtree discretization, Barnes and Lumley (2011) were able to jointly process multiple components of airborne gravity-gradient data using a single layer of equivalent sources. To our knowledge, Barnes and Lumley (2011) are the pioneers on processing full-tensor gravity-gradient data jointly. In addition to computational feasibility, Barnes and Lumley's (2011) method reduces low-frequency noise and can also remove the drift in time-domain from the survey data. Those authors stressed that the $G_{zz}-$component calculated through the single estimated equivalent-layer model projected on a grid at a constant elevation by inverting full gravity-gradient data has the low-frequency error reduced by a factor of 2.4 as compared to the inversion of an individual component of the gravity-gradient data.

2.2.5 The reparametrization of the equivalent layer

Oliveira Jr. et al. (2013) reparametrized the whole equivalent-layer model by a piecewise bivariate-polynomial function defined on a set of equivalent-source windows. By using a regularized potential-field inversion, Oliveira Jr. et al. (2013) estimates the polynomial coefficients for each equivalent-source window. After estimating all polynomial coefficients of all windows, the estimated coefficients are transformed into a single physical-property distribution encompassing the entire equivalent layer. This approach was called "polynomial equivalent layer". As stated by Oliveira Jr. et al. (2013), the computational efficiency of polynomial equivalent layer stems from the fact that the total number of polynomial coefficients required to depict the physical-property distribution within the equivalent layer is generally much smaller than the number of equivalent sources. Consequently, this leads to a considerably smaller linear system that needs to be solved. Hence, the main strategy of polynomial equivalent layer is the model dimension reduction.

The polynomial equivalent layer was applied to perform upward continuations of gravity and magnetic data and reduction to the pole of magnetic data.

2.2.6 The iterative scheme without solving a linear system

There exists a class of methods that iteratively estimate the distribution of physical properties within an equivalent layer without the need to solve linear systems. The method initially introduced by Cordell (1992) and later expanded upon by Guspí and Novara (2009) updates the physical property of sources, located beneath each potential-field data, by removing the maximum residual between the observed and fitted data. In addition, Xia and Sprowl (1991) and Xia et al. (1993) have developed efficient iterative algorithms for updating the distribution of physical properties within the equivalent layer in the wavenumber and space domains, respectively. Specifically, in Xia and Sprowl's (1991) method the physical-property distribution is updated by using the ratio between the squared depth to the equivalent source and the gravitational constant multiplied by the residual between the observed and predicted observation at the measurement station. Neither of these methods solve linear systems.

Following this class of methods of iterative equivalent-layer technique that does not solve linear systems, Siqueira et al. (2017) developed a fast iterative equivalent-layer technique for processing gravity data in which the sensitivity matrix $\mathbf{A}$ (equation 1) is replaced by a diagonal matrix $N \times N$, i.e.:

$$\tilde{\tilde{\mathbf{A}}} = 2\,\pi\,\gamma\,\mathbf{\Delta S^{-1}}\,, \tag{7}$$

where γ is Newton's gravitational constant and $\mathbf{\Delta S^{-1}}$ is a diagonal matrix of order N whose diagonal elements Δs_i, $i = 1, ..., N$ are the element of area centered at the ith horizontal coordinates of the ith observation point. The physical foundations of Siqueira et al.'s (2017) method rely on two constraints: i) the excess of mass; and ii) the positive correlation between the gravity observations and the mass distribution over the equivalent layer. By starting from a mass distribution on the equivalent layer, whose ith mass p_i^o is proportional to the ith observed $\mathbf{g_z}$-component data d_i^o,

$$p_i^o = \frac{\Delta s_i\, d_i^o}{2\,\pi\,\gamma}\,, \tag{8}$$

Siqueira et al.'s (2017) method updates the mass distribution by adding mass corrections that are proportional to the data residuals. At the kth iteration, the ith mass correction is given by:

$$\Delta\hat{p}^k{}_i = \frac{\Delta s_i\, r_i^k}{2\,\pi\,\gamma}\,, \tag{9}$$

where the ith data residual r_i^k is computed by subtracting the observed d_i^o from the fitted $\mathbf{g_z}$-component data d_i^k at the kth iteration, i.e.:

$$r_i^k = d_i^o\; -\; d_i^k\,. \tag{10}$$

Siqueira et al. (2017) applied their fast iterative equivalent-layer technique to interpolate, calculate the horizontal components, and continue upward (or downward) gravity data.

For jointly process two gravity gradient components, Jirigalatu and Ebbing (2019) used the Gauss-FFT for forward calculation of potential fields in the wavenumber domain combined with Landweber's iteration coupled with a mask matrix $\mathbf{M}$ to reduce the edge effects without increasing the computation cost. The mask matrix $\mathbf{M}$ is defined in the following way: if the corresponding pixel does not contain the original data, the element of $\mathbf{M}$ is set to zero; otherwise, it is set to one. The kth Landweber iteration is given by

$$\mathbf{p}_{k+1} = \mathbf{p}_k + \omega \left[\mathbf{A_1}^\top (\mathbf{d_1} - \mathbf{M}\mathbf{A_1}\mathbf{p}_k) + \mathbf{A_2}^\top (\mathbf{d_2} - \mathbf{M}\mathbf{A_2}\mathbf{p}_k) \right] \;, \tag{11}$$

where ω is a relaxation factor, $\mathbf{d_1}$ and $\mathbf{d_2}$ are the two gravity gradient components and $\mathbf{A_1}$ and $\mathbf{A_2}$ are the corresponding gravity gradient kernels. Jirigalatu and Ebbing (2019) applied their method for processing two horizontal curvature components of Falcon airborne gravity gradient.

2.2.7 The convolutional equivalent layer with BTTB matrices

Takahashi et al. (2020, 2022) introduced the convolutional equivalent layer for gravimetric and magnetic data processing, respectively.

Takahashi et al. (2020) demonstrated that the sensitivity matrix $\mathbf{A}$ (equation 1) associated with a planar equivalent layer formed by a set of point masses, each one directly beneath each observation point and considering a regular grid of observation points at a constant height has a symmetric block-Toeplitz Toeplitz-block (BTTB) structure. A symmetric BTTB matrix has, at least, two attractive properties. The first one is that it can be defined by using only the elements forming its first column (or row). The second attractive property is that any BTTB matrix can be embedded into a symmetric Block-Circulat Circulant-Block (BCCB) matrix. This means that the full sensitivity matrix $\mathbf{A}$ (equation 1) can be completely reconstruct by using the first column of the BCCB matrix only. In what follows, Takahashi et al. (2020) computed the forward modeling by using only a single equivalent source. Specifically, it is done by calculating the eigenvalues of the BCCB matrix that can be efficiently computed by using only the first column of the BCCB matrix via 2D fast Fourier transform (2D FFT). By comparing with the classic approach in the Fourier domain, the convolutional equivalent layer for gravimetric data processing proposed by Takahashi et al. (2020) performed upward- and downward-continue gravity data with a very small border effects and noise amplification.

By using the original idea of the convolutional equivalent layer proposed by Takahashi et al. (2020) for gravimetric data processing, Takahashi et al. (2022) proposed the convolutional equivalent layer for magnetic data processing. By assuming a regularly spaced grid of magnetic data at a constant height and a planar equivalent layer of dipoles, Takahashi et al. (2022) proved that the sensitivity matrix linked with this layer possess a BTTB structure in the specific scenario where each dipole is exactly beneath each observed magnetic data point. Takahashi et al. (2022) used a conjugate gradient algorithm (CGLS) which does not require an inverse matrix or matrix-matrix multiplication. Rather, it only requires matrix-vector multiplications per iteration, which can be effectively computed using the 2D FFT as a discrete convolution. The matrix-vector product only uses the elements that constitute the first column of the associated BTTB matrix, resulting in computational time and memory savings. Takahashi et al. (2022) showed the robustness of the convolutional equivalent layer in processing magnetic survey that violates the requirement of regular grids in the horizontal directions and flat observation surfaces. The convolutional equivalent layer was applied to perform upward continuation of large magnetic datasets. Compared to the classical Fourier approach, Takahashi et al.'s (2022) method produces smaller border effects without using any padding scheme.

Without taking advantage of the symmetric BTTB structure of the sensitivity matrix (Takahashi et al., 2020) that arises when gravimetric observations are measured on a horizontally regular grid, on a flat surface and considering a regular grid of equivalent sources whithin a horizontal layer, Mendonça (2020) explored the symmetry of the gravity kernel to reduce the number of forward model evaluations. By exploting the symmetries of the gravity kernels and redundancies in the forward model evaluations on a regular grid and combining the subspace solution based on eigenvectors of the gridded dataset, Mendonça (2020) estimated the mass excess or deficiency produced by anomalous sources with positive or negative density contrast.

3 NUMERICAL SIMULATIONS

We investigated different computational algorithms for inverting gravity disturbances and total-field anomalies. To test the capability of the fast equivalent-layer technique for processing that potential field data, we construct two tests. The first one is a measure of the computational effort by counting the number of floating-point operations (*flops*), such as additions, subtractions, multiplications, and divisions (Golub and Loan, 2013). Secondly, we demonstrated the solution stability by using a zeroth-order Tikhonov regularization in different noise levels. Finally, we show two examples of gravity and magnetic data processing.

For all applications, we generate a model composed by two spheres (PAREI AQUI - ANDRE)

3.1 Floating-point operations calculation

To measure the computational effort of the different algorithms to solve the equivalent layer linear system, a non-hardware dependent method can be useful because allow us to do direct comparison between them. Counting the floating-point operations (*flops*), i.e., additions, subtractions, multiplications and divisions is a good way to quantify the amount of work of a given algorithm (Golub and Loan, 2013). For example, the number of *flops* necessary to multiply two vectors $\mathbb{R}^N$ is $2N$. A common matrix-vector multiplication with dimension $\mathbb{R}^{N\times N}$ and $\mathbb{R}^N$, respectively, is $2N^2$ and a multiplication of two matrices $\mathbb{R}^{N\times N}$ is $2N^3$. Figure XX shows the total flops count for the different methods presented in this review with a crescent number of data, ranging from $10,000$ to $1,000,000$.

3.1.1 Normal equations using Cholesky decomposition

The equivalent sources can be estimated directly from solving the normal equations 1. In this work we will use the Cholesky decompositions method to calculate the necessary *flops*. In this method it is calculated the lower triangule of $\mathbf{A}^T\mathbf{A}$ $(1/2N^3)$, the Cholesky factor $(1/3N^3)$, a matrix-vector multiplication $(2N^2)$ and finally solving the triangular system $(2N^2)$, totalizing

$$f_{classical} = \frac{5}{6}N^3 + 4N^2 \tag{12}$$

3.1.2 Window method (Leão and Silva, 1989)

The moving data-window scheme (Leão and Silva, 1989) solve N linear systems with much smaller sizes. For our results we are considering a data-window of the same size of wich the authors presented in theirs work $(N_w = 49)$ but, calculating with the same number of equivalent sources and not only the one in the middle of the window. We are doing this process for all the other techniques to standardize the resolution of our problem. Using the Cholesky decomposition with this method the *flops* are

$$f_{window} = N\frac{5}{6}N_w^3 + 4N_w^2 \tag{13}$$

3.1.3 PEL method (Oliveira Jr. et al., 2013)

The polynomial equivalent layer uses a simliar approach od moving windows from Leão and Silva (1989). For this operations calculation we used a first degree polynomial (three variables) and each window contains $1,000$ observed data (N_s). Following the steps given in (Oliveira Jr. et al., 2013) the total *flops* becomes

$$f_{pel} = \frac{1}{3}H^3 + 2H^2 + 2NN_wH + H^2N + 2HN + 2NP \tag{14}$$

where H is the number of variable of the polynomial times the number of windows ($3 \times N/1000$).

3.1.4 Conjugate gradient least square (CGLS)

The CGLS method is a very stable and fast algorithm for solving linear systems iteratively. Its computational complexity envolves a matrix-vector product outside the loop ($2N^2$), two matrix-vector products inside the loop ($4N^2$) and six vector products inside the loop ($12N$)

$$f_{cgls} = 2N^2 + it(4N^2 + 12N) \tag{15}$$

3.1.5 Wavelet compression method with CGLS (Li and Oldenburg, 2010)

For the wavelet method we have calculated a coompression rate C_r of 98% of threshold as the authors in Li and Oldenburg (2010) used and the wavelet transformation requiring $\log_2(N)$ *flops* each, with its inverse also using the same number of operations. Combined with the conjugate gradient least square necessary steps and iterations, the number of *flops* are

$$f_{wavelet} = 2NC_r + 4N\log_2(N) + it(4N\log_2(N) + 4NC_r + 12C_r) \tag{16}$$

3.1.6 Convolutional equivalent layer for gravity data (Takahashi et al., 2020)

This methods replaces the matrix-vector multiplication of the iterative fast-equivalent technique (Siqueira et al., 2017) by three steps involving a Fourier transform and a inverse Fourier transform, and a Hadamard product of matrices. Considering that the first column of our BCCB matrix has $4N$ elements, the flops count of this method is

$$f_{convgrav} = \kappa 4N\log_2(4N) + it(27N + \kappa 8N\log_2(4N)) \tag{17}$$

In the resultant count we considered a *radix-2* algorithm for the fast Fourier transform and its inverse, which has a κ equals to 5 and requires $\kappa 4N\log_2(4N)$ flops each. The Hadarmard product of two matrices of $4N$ elements with complex numbers takes $24N$ flops. Note that equation 17 is different from the one presented in Takahashi et al. (2020) because we also added the flops necessary to calculate the eigenvalues in this form. It does not differentiate much in order of magnitude because the iterative part is the most costful.

3.1.7 Convolutional equivalent layer for magnetic data (Takahashi et al., 2022)

The convolutional equivalent layer for magnetic data uses the same flops count of the main operations as in the gravimetric case, the big difference is the use of the conjugate gradient algorithm to solve the inverse problem. It requires a Hadamard product outside of the iterative loop and more matrix-vector vector-vector multiplications inside the loop as seem in equation 15.

$$f_{convmag} = \kappa 16N\log_2(4N) + 24N + it(\kappa 16N\log_2(4N) + 60N) \tag{18}$$

3.1.8 Deconvolutional method

The deconvolution method does not require an iterative algorithm, rather it solves the estimative of the physical properties in a single step using the $4N$ eigenvalues of the BCCB matrix as in the convolutional method. It requires a two fast Fourier transform ($\kappa 4N \log_2(4N)$), one for the eigenvalues and another for the data transformation, a element by element division ($24N$) and finally, a fast inverse Fourier transform for the final estimative ($\kappa 4N \log_2(4N)$).

$$f_{deconv} = \kappa 12N \log_2(4N) + 24N \tag{19}$$

Using the deconvolutional method with a Wiener stabilization adds two multiplications of complex elements of the conjugates eigenvalues ($24N$ each) and the sum of $4N$ elements with the stabilization parameter μ

$$f_{deconvwiener} = \kappa 12N \log_2(4N) + 76N \tag{20}$$

3.2 Stability analysis

For the stability analysis we show the comparison of the normal equations solution with zeroth-order Tikhonov regularization, the convolutional method for gravimetric and magnetic data, the deconvolutional method and the deconvolutional method with different values for the Wiener stabilization. We create 21 data sets adding a crescent pseudo-random noise to the original data, which varies from 0% to 10% of the maximum anomaly value, in intervals of 0.5%. These noises has mean equal to zero and a Gaussian distribution. Figure XX shows how the residual between the predicted data and the noise-free data changes as the level of the noise is increased. We can see that for all methods, a linear tendency can be observed as it is expected. The inclination of the straight line is a indicative of the stability of each method. As show in the graph the deconvolutional method is very unstable and it is really necessary to use a stabilization method to have a good parameter estimative. In contrast, a correct value of the stabilization parameter is necessary to not overshoot the smootheness of the solution as it is the case for the well-known zeroth-order Tikhonov regularization. For the example using this gravimetric data, the optimal value for the Wiener stabilization parameter is $\mu = 10^{-9}$. Figure XX shows the comparison of the predicted data for each method with the original data.

For the magnetic data, the Wiener parameter seems to have the best solution for $\mu = 10^{-13}$. Figure XX shows the comparison of the predicted data for each method with the original data.

4 DISCUSSION AND CONCLUSION

CONFLICT OF INTEREST STATEMENT

The authors declare that the research was conducted in the absence of any commercial or financial relationships that could be construed as a potential conflict of interest.

AUTHOR CONTRIBUTIONS

The Author Contributions section is mandatory for all articles, including articles by sole authors. If an appropriate statement is not provided on submission, a standard one will be inserted during the production process. The Author Contributions statement must describe the contributions of individual authors referred to by their initials and, in doing so, all authors agree to be accountable for the content of the work. Please see here for full authorship criteria.

FUNDING

Diego Takahashi was supported by a Post-doctoral scholarship from CNPq (grant 300809/2022-0) Valéria C.F. Barbosa was supported by fellowships from CNPq (grant 309624/2021-5) and FAPERJ (grant 26/202.582/2019). Vanderlei C. Oliveira Jr. was supported by fellowships from CNPq (grant 315768/2020-7) and FAPERJ (grant E-26/202.729/2018).

ACKNOWLEDGMENTS

We thank the brazillian federal agencies CAPES, CNPq, state agency FAPERJ and Observatório Nacional research institute and Universidade do Estado do Rio de Janeiro.

DATA AVAILABILITY STATEMENT

The datasets generated for this study can be found in the frontiers-paper Github repository link: https://github.com/DiegoTaka/frontiers-paper.

REFERENCES

Aster, R. C., Borchers, B., and Thurber, C. H. (2018). *Parameter estimation and inverse problems* (Elsevier)

Barbosa, V. C. F., Silva, J. B., and Medeiros, W. E. (1997). Gravity inversion of basement relief using approximate equality constraints on depths. *Geophysics* 62, 1745–1757

Barnes, G. and Lumley, J. (2011). Processing gravity gradient data. *Geophysics* 76, I33–I47. doi:10.1190/1.3548548

Cordell, L. (1992). A scattered equivalent-source method for interpolation and gridding of potential-field data in three dimensions. *Geophysics* 57, 629–636

Dampney, C. N. G. (1969). The equivalent source technique. *Geophysics* 34, 39–53. doi:10.1190/1.1439996

Davis, K. and Li, Y. (2011). Fast solution of geophysical inversion using adaptive mesh, space-filling curves and wavelet compression. *Geophysical Journal International* 185, 157–166. doi:10.1111/j.1365-246X.2011.04929.x

Friedman, J. H. (2001). Greedy function approximation: a gradient boosting machine. *Annals of statistics* , 1189–1232

Friedman, J. H. (2002). Stochastic gradient boosting. *Computational statistics and data analysis* 38, 367–378

Golub, G. H. and Loan, C. F. V. (2013). *Matrix Computations (Johns Hopkins Studies in the Mathematical Sciences)* (Johns Hopkins University Press), 4 edn.

Guspí, F. and Novara, I. (2009). Reduction to the pole and transformations of scattered magnetic data using newtonian equivalent sources. *Geophysics* 74, L67–L73

Jirigalatu, J. and Ebbing (2019). A fast equivalent source method for airborne gravity gradient data. *Geophysics* 84, G75–G82. doi:10.1190/GEO2018-0366.1

Kellogg, O. D. (1929). *Foundations of Potential Theory* (Frederick Ungar Publishing Company)

Kennett, B., Sambridge, M., and Williamson, P. (1988). Subspace methods for large inverse problems with multiple parameter classes. *Geophysical Journal International* 94, 237–247

Leão, J. W. D. and Silva, J. B. C. (1989). Discrete linear transformations of potential field data. *Geophysics* 54, 497–507. doi:10.1190/1.1442676

Li, Y. and Oldenburg, D. W. (2010). Rapid construction of equivalent sources using wavelets. *Geophysics* 75, L51–L59. doi:10.1190/1.3378764

Mendonça, C. A. (2020). Subspace method for solving large-scale equivalent layer and density mapping problems. *Geophysics* 85, G57–G68. doi:10.1190/geo2019-0302.1

Mendonça, C. A. and Silva, J. B. C. (1994). The equivalent data concept applied to the interpolation of potential field data. *Geophysics* 59, 722–732. doi:10.1190/1.1443630

Oldenburg, D., McGillivray, P., and Ellis, R. (1993). Generalized subspace methods for large-scale inverse problems. *Geophysical Journal International* 114, 12–20

Oliveira Jr., V. C., Barbosa, V. C. F., and Uieda, L. (2013). Polynomial equivalent layer. *Geophysics* 78, G1–G13. doi:10.1190/geo2012-0196.1

Siqueira, F. C., Oliveira Jr, V. C., and Barbosa, V. C. (2017). Fast iterative equivalent-layer technique for gravity data processing: A method grounded on excess mass constraint. *Geophysics* 82, G57–G69

Skilling, J. and Bryan, R. (1984). Maximum entropy image reconstruction-general algorithm. *Monthly Notices of the Royal Astronomical Society, Vol. 211, NO. 1, P. 111, 1984* 211, 111

Soler, S. R. and Uieda, L. (2021). Gradient-boosted equivalent sources. *Geophysical Journal International* 227, 1768–1783. doi:10.1093/gji/ggab297

Takahashi, D., Oliveira, V. C., and Barbosa, V. C. (2022). Convolutional equivalent layer for magnetic data processing. *Geophysics* 87, 1–59

Takahashi, D., Oliveira Jr, V. C., and Barbosa, V. C. (2020). Convolutional equivalent layer for gravity data processing. *Geophysics* 85, G129–G141

Xia, J. and Sprowl, D. R. (1991). Correction of topographic distortion in gravity data. *Geophysics* 56, 537–541

Xia, J., Sprowl, D. R., and Adkins-Heljeson, D. (1993). Correction of topographic distortions in potential-field data; a fast and accurate approach. *Geophysics* 58, 515–523. doi:10.1190/1.1443434

5 SUPPLEMENTARY TABLES AND FIGURES

476 ## 5.1 Figures

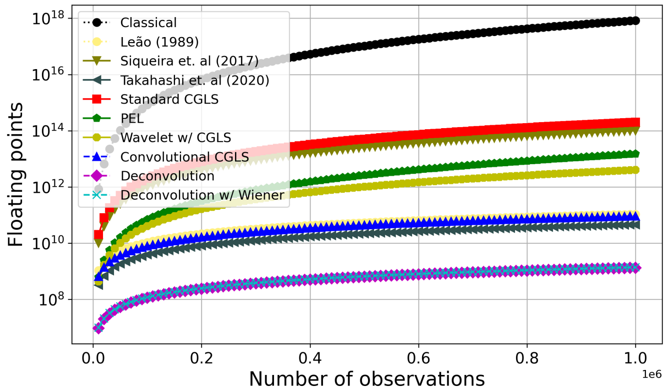

Figure 1. Number of *flops* for some of the methods to estimate the equivalent sources of the gravimetric case.

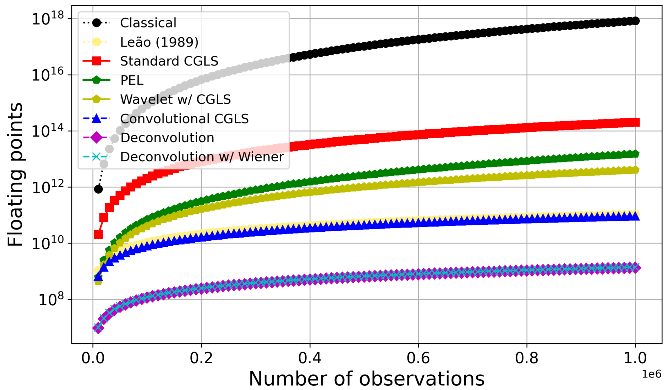

Figure 2. Number of *flops* for some of the methods to estimate the equivalent sources of the magnetic case.

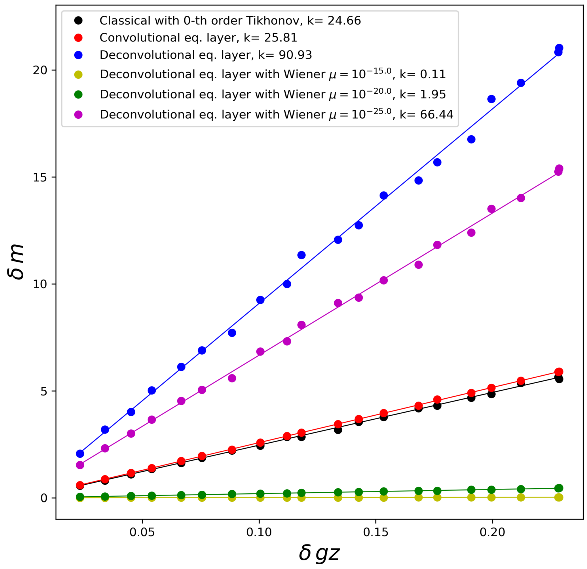

Figure 3. Stability analysis of some of the equivalent layer methods of the gravimetric case.

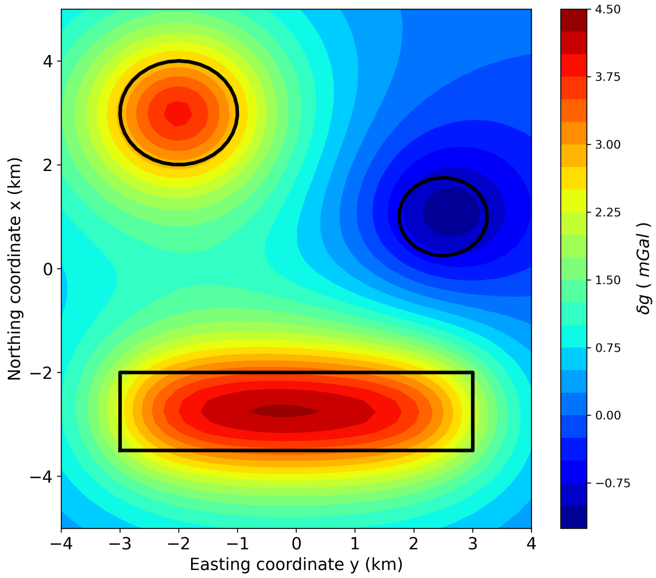

Figure 4. Synthetic noise-free data of the gravimetric case.

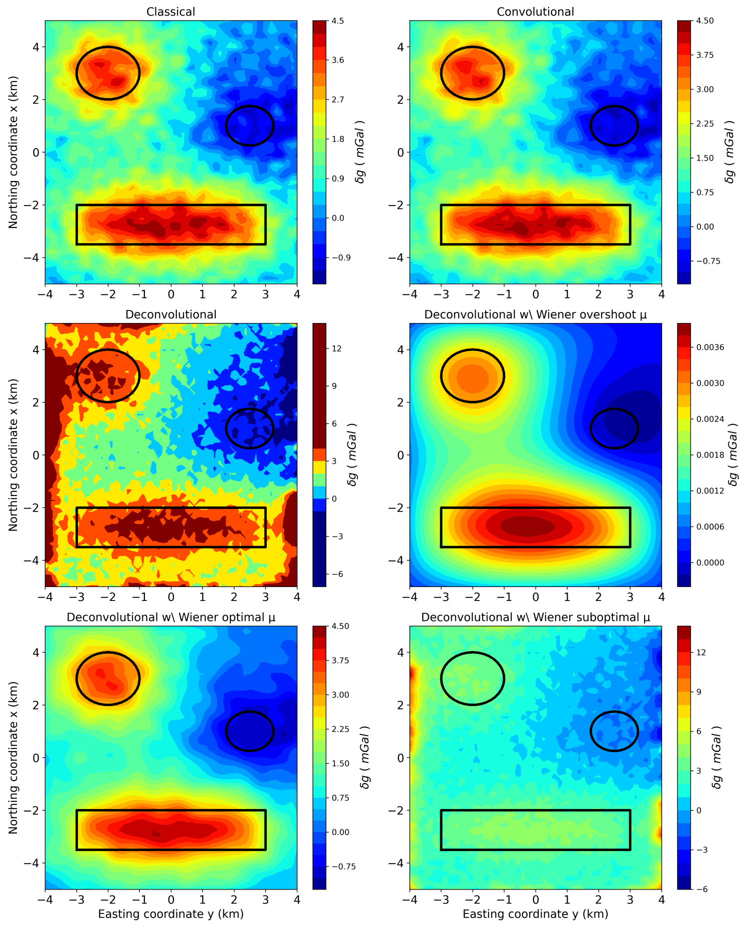

Figure 5. Predicted gravity data for different methods of the equivalent layer with maximum level of noise. Panel **(A)** is the classical method, **(B)** is the convolutional, **(C)** is the deconvolutional, **(D)** is the deconvolutional method using Wiener stabilization with a too high value for μ, **(E)** is the deconvolutional method using Wiener stabilization with a optimal value for μ and **(F)** is the deconvolutional method using Wiener stabilization with a too low value for μ.

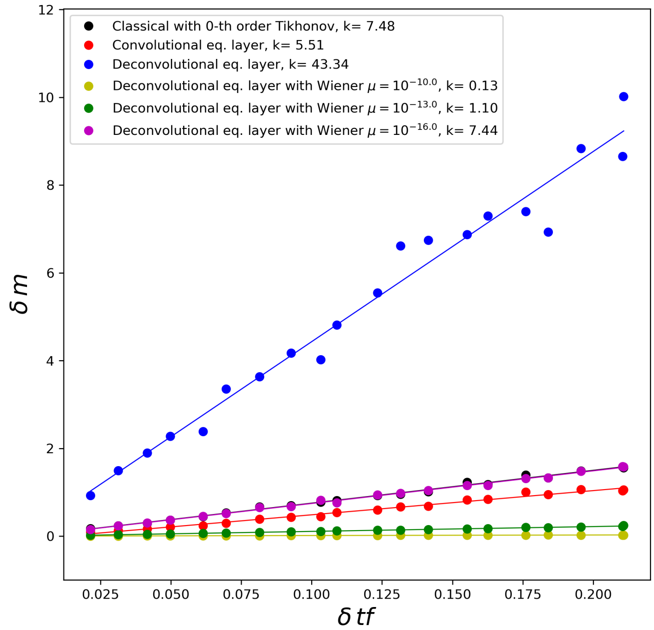

Figure 6. Stability analysis of some of the equivalent layer methods of the magnetic case.

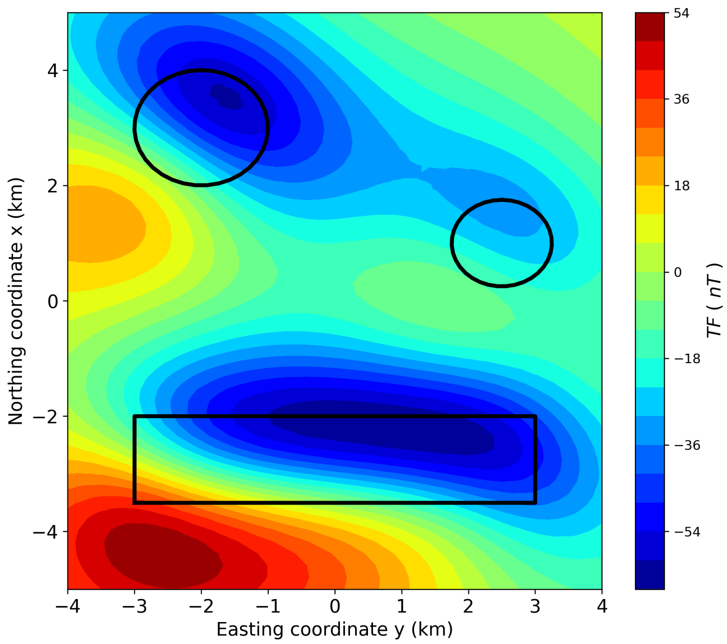

Figure 7. Synthetic noise-free data of the magnetic case.

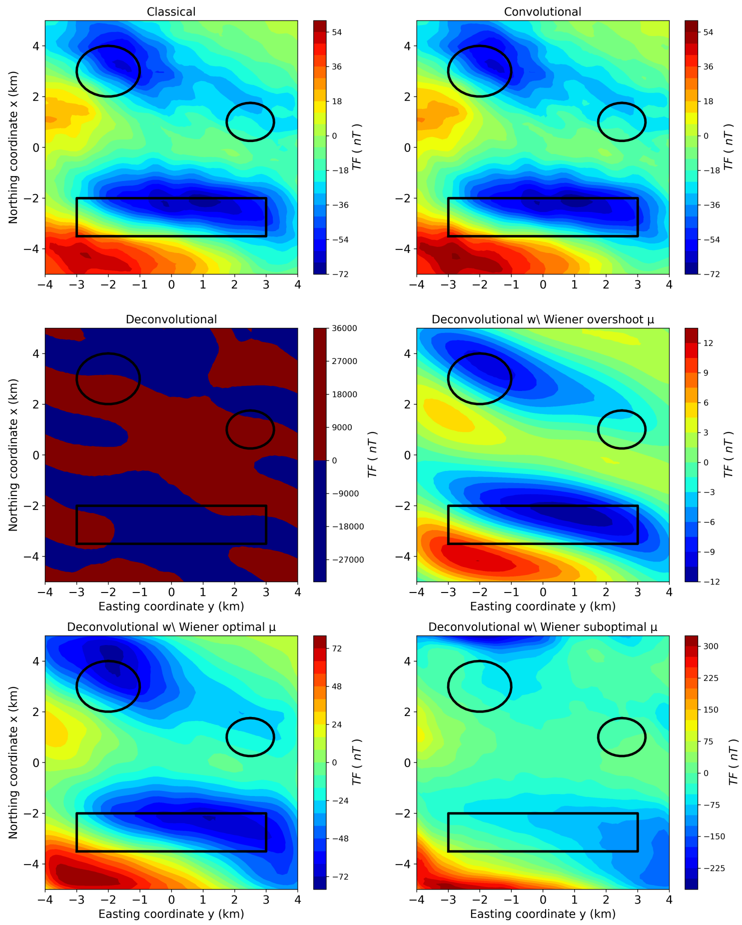

Classical
Convolutional
Deconvolutional
Deconvolutional w\ Wiener overshoot μ
Deconvolutional w\ Wiener optimal μ
Deconvolutional w\ Wiener suboptimal μ
Northing coordinate x (km)
Easting coordinate y (km)
TF (nT)

Figure 8.